

https://dspace.org/

A carboxymethyl cellulase from the yeast Crytococcus gattii WM276 Expression purification and characterisation

Dylan Moodley; Angela Botes

ACADEMIC PRESS INC ELSEVIER SCIENCE
https://hdl.handle.net/10539/45615
WOS

Downloaded from a DSpace repository. https://dspace.org/

Protein Expression and Purification 225 (2025) 106594

Contents lists available at ScienceDirect

Protein Expression and Purification

journal homepage: www.elsevier.com/locate/yprep

Research Article

A carboxymethyl cellulase from the yeast *Cryptococcus gattii* WM276: Expression, purification and characterisation

Dylan Moodley, Angela Botes *

School of Molecular and Cell Biology, University of the Witwatersrand, Johannesburg, South Africa

ARTICLE INFO

Keywords:
Cryptococcus gattii
Cellulase
MBP
Fusion enzyme

ABSTRACT

Cryptococcus gattii and its medical implications have been extensively studied. There is, however, a significant knowledge gap regarding cryptococcal survival in its environmental niche, namely woody material, which is glaring given that infection is linked to environmental populations. A gene from *C. gattii* (WM276), the predominant global molecular type (VGI), has been sequenced and annotated as a putative cellulase. It is therefore, of both medical and industrial intertest to delineate the structure and function of this enzyme. A homology model of the enzyme was constructed as a fusion protein to a maltose binding protein (MBP). The CGB_E4160W gene was overexpressed as an MBP fusion enzyme in *Escherichia coli* T7 cells and purified to homogeneity using amylose affinity chromatography. The structural and functional character of the enzyme was investigated using fluorescence spectroscopy and enzyme activity assays, respectively. The optimal enzyme pH and temperature were found to be 6.0 and 50 °C, respectively, with an optimal salt concentration of 500 mM. Secondary structure analysis using Far-UV CD reveals that the MBP fusion protein is primarily α-helical with some β-sheets. Intrinsic tryptophan fluorescence illustrates that the MBP-cellulase undergoes a conformational change in the presence of its substrate, CMC-Na^+. The thermotolerant and halotolerant nature of this particular cellulase, makes it useful for industrial applications, and adds to our understanding of the pathogen's environmental physiology.

1. Introduction

Cryptococcus gattii is a yeast pathogen that has been repeatedly isolated from various environmental sources including guano, soil, and particularly, woody material [1,2]. Along with its sister species, *Cryptococcus neoformans*, *C. gattii* is associated with lethal infections in both animals and humans. Whilst the medical implications surrounding *C. gattii* have been extensively scrutinized over the decades [3,4], its environmental capabilities and physiology on woody material remain poorly understood. Like other Tremellales fungi, *C. gattii* is often isolated from soil and decaying woody material, particularly woody material that has a waxy texture, such as *Eucalyptus camaldulensis*, *Pseudotsuga menziesii* and *Prunus dulcis* trees [5–7]. When considering that *C. gattii* has been routinely isolated from decaying woody material [5,7–9], it would not be unlikely that *C. gattii* is capable of utilizing lignocellulosic material as a potential carbon source. This hypothesis is corroborated by the fact that the closely related *C. neoformans* was previously reported to use carboxymethyl cellulose (CMC) as a sole carbon source, likely due to cellulolytic activity, [10]. Moreover, *C. gattii* is known to produce a laccase enzyme, whose function has been implicated in lignin hydrolysis due to its ability to catalyse the oxidation of phenolic components within lignocellulosic material [11,12].

Lignocellulosic biomass is considered the most abundantly available biopolymer and source of potential renewable energy on Earth [13,14]. Numerous sources of lignocellulosic material exist, including sugarcane bagasse, paper waste from the paper industry, cereal straw, maize stover, and agricultural wastes such as empty fruit and vegetable tree branches [15]. Lignocellulosic is a complex polymer composed of the polysaccharides cellulose and hemicellulose; as well as the aromatic polymer lignin [14]. Cellulose, a linear homopolymeric polysaccharide, consists of repeating units of dextrorotatory glucose (D-glucose) and accounts for 40–60 % of lignocellulose [16]. Enzymatic hydrolysis is achieved through the use of cellulases [17], which have found wide application in agriculture, industry, and medicine [18]. The hydrolytic mechanism of cellulases varies depending on the site of catalysis, with endocellulases acting on amorphous regions of cellulose [19], while exocellulases sequentially cleave linkages from either the reducing end (type I) or non-reducing end (type II) of the cellulosic chain [17].

As such, the aim of this research is the characterization of a putative *C. gattii* cellulase that will provide insight into the environmental metabolism of this yeast pathogen with regards to plant colonization

* Corresponding author.
E-mail address: angela.botes@wits.ac.za (A. Botes).

https://doi.org/10.1016/j.pep.2024.106594
Received 8 May 2024; Received in revised form 21 August 2024; Accepted 25 August 2024
Available online 26 August 2024
1046-5928/© 2024 The Authors. Published by Elsevier Inc. This is an open access article under the CC BY-NC-ND license (http://creativecommons.org/licenses/by-nc-nd/4.0/).

Abbreviations

Cryptococcus gattii *C. gattii*
MBP Maltose binding protein
Far-UV CD Far-ultraviolet circular dichroism
CMC-Na^+ Carboxymethyl cellulose-sodium salt

and ultimately human infection.

2. Materials and methods

2.1. Vector construction

The putative cellulase gene sequence CGB_E4160W (923 nucleotides/307 amino acids [accession number: XM_003194284]), originating from the genome of *C. gattii* WM276, was submitted to GenScript Inc, Piscataway, NJ, USA, where the sequence was codon optimized for *Escherichia coli* and cloned into the expression vector system pMAL-c5x using *Nde*I and *Eco*RI restriction sites, generating pMAL-CGB_E4160W. *Cryptococcus gattii* WM276 represents the predominant global molecular type (VGI), and was originally isolated from the Australian environment [20].

2.2. Protein bioinformatics

In silico analysis of the recombinant cellulase from *C. gattii* was carried out using ProtParam in order to delineate the theoretical character of the cellulase in terms of its isoelectric point (pI), theoretical molecular weight, instability index (which is often correlated to the *in vivo* half-life of a protein) [21], grand average of hydropathicity (GRAVY) (a determinant of solubility in a recombinant host) and molar extinction coefficient [22].

To determine the presence or absence of a signal peptide, SignalP (version 5; https://services.healthtech.dtu.dk/service.php?SignalP-5.0), in conjunction with Phobius (version 1; https://phobius.sbc.su.se/) and Predisi (version 1; http://www.predisi.de/), were used with the native amino acid sequence as the input to determine these parameters.

An automated homology model, using maltose binding protein-cellulase's amino acid sequence as the input, was constructed using the Phyre2 web portal (http://www.sbg.bio.ic.ac.uk/phyre2) for protein modelling. Structure prediction and analysis were carried out using the software's 'intensive' mode. The intensive mode of Phyre2 aims to construct a comprehensive full-length homology model of a given amino acid sequence by combining multiple template models with simplified *ab initio* folding simulations [23]. The homology model was subsequently visualized using PyMOL [24].

2.3. Recombinant protein overexpression and purification

Escherichia coli T7 cells were transformed with the pMAL-CGB_E4160W vector [25]. Single colonies were cultured overnight in Luria-Bertani (LB) broth (pH 7), supplemented with 100 μg ampicillin ml^{-1}, at 37 °C with shaking at 200 rpm. The overnight cultures were diluted 1/10 with fresh LB broth supplemented with 100 μg ampicillin ml^{-1} at 37 °C with shaking at 200 rpm until the OD_{600} was approximately 0.35–0.55. The cultures were induced with isopropyl β-D-1-thiogalactopyranoside (IPTG) at a final concentration of 0.2 mM and cultured for an additional 24 h at 16 °C with shaking at 200 rpm. Cells were subsequently harvested by centrifugation (4000×*g*, 20 min, 4 °C). Approximately 1 g of wet cell pellet was obtained per 100 mL, and the pellet was resuspended in 10 mL lysis buffer (20 mM Tris-HCl; 200 mM NaCl; pH 7.4). The resuspended cells were sonicated (QSonica Q125; 60 % amplitude; 8 cycles of 30 s ultrasonic pulses followed by 30 s on ice) to disrupt the bacterial cell wall. The soluble extracts were separated from the insoluble cell debris via centrifugation at 20 000×*g* for 15 min at 4 °C. The soluble extracts were assayed using sodium dodecyl sulphate–polyacrylamide gel electrophoresis (SDS-PAGE) to verify the production of soluble maltose binding protein (MBP)-cellulase (~90 kDa) [26].

In order to purify the MBP-cellulase, an amylose column was pre-equilibrated with 15 column volumes of amylose affinity binding buffer (20 mM Tris-HCl; 200 mM NaCl; pH 7.4). The soluble extracts were clarified with a 0.22 μm syringe filter and subsequently diluted in excess amylose affinity binding buffer in a 1:5 ratio to increase the contact time between the resin and maximise binding of the MBP-cellulase within the soluble extracts. The diluted soluble extracts were added to the column, after which the column was washed with 25 column volumes of amylose affinity binding buffer to remove any non-specifically bound material. The immobilised MBP-cellulase fusion protein was eluted using amylose affinity elution buffer (20 mM Tris-HCl; 200 mM NaCl; 10 mM maltose; pH 7.4) All chromatographic fractions were assayed using SDS-PAGE to qualitatively determine the purity of the MBP-cellulase fusion protein.

2.4. Far-ultraviolet circular dichroism (Far-UV CD) and intrinsic tryptophan fluorescence

A total of 10 μM MBP-cellulase, which was dialysed against 20 mM sodium phosphate buffer (pH 7.4) for 24 h in order to remove any salts which would have hampered accurate spectroscopic measurements [27], was subjected to far-UV CD analysis. The following parameters were set for CD spectra collection on a Jasco J-810 Circular Dichroism Spectropolarimeter: sensitivity (100 mdeg), start wavelength (260 nm), end wavelength (190 nm), data pitch (0.5 nm), scanning mode (continuous), scanning speed (1000 nm/s), response (1 s) and bandwidth (5 nm) [28]. A blank containing only sodium phosphate buffer (20 mM; pH 7.4) was also assessed to obtain the contribution of the buffer to the CD spectrum. The CD spectrofluorometer's output data is in ellipticity units ([θ]) and a total of five readings were recorded. The data was then converted into mean residual ellipticity [θ]MWR with the equation:

$$[\theta] = \frac{(100 \times \theta)}{C \times n \times l}$$

θ = ellipticity (mdeg)
n = number of amino acid residues
l = path length (1 mm)
c = protein concentration (g/ml)

MBP-cellulase was subjected to intrinsic tryptophan fluorescence in order to study MBP-cellulase's conformational changes when in the presence of its ligand, CMC-Na^+, and when denatured in 8 M urea. A total of 10 μM MBP-cellulase in 10 mM sodium phosphate buffer (pH 7) was used in the analysis of native MBP-cellulase, whilst 10 mM sodium phosphate buffer (pH 7) supplemented with 8 M urea was used in the analysis of denatured MBP-cellulase and 10 mM sodium phosphate buffer (pH 7) supplemented with 0.5 % (w/v) CMC-Na^+ was used in the analysis of ligand-bound MBP-cellulase. The resultant difference in tryptophan spectra and intensity under three varying conditions was assessed, specifically, the native, denatured and ligand-bound state of MBP-cellulase. The observation of a blue- or red-shift was observed, depending on the initial degree of quenching. All samples were analysed using the Jasco FP-8200 spectrofluorometer with the following settings: excitation bandwidth (2.5 nm), emission bandwidth (5 nm), the response time (1 s), sensitivity (high), excitation wavelength (295 nm), measurement range (280–500 nm) and data interval (200 nm/min) with three accumulations. Background noise was corrected for by subtracting

background buffer values from the actual MBP-cellulase spectra.

2.5. Assaying soluble extracts for cellulase activity

The cellulolytic capabilities of the recombinant MBP-cellulase were confirmed using a standard DNS (3,5-dinitrosalicylic acid) assay [29]. A total 250 μg of soluble protein extracts were incubated in the presence of 1 mL 0.5 % (w/v) CMC-Na^+ in 50 mM sodium phosphate buffer (pH 6) for 1 h at 50 °C. The addition of 3 mL DNS reagent (2 % w/v DNS; 0.5 M NaOH; 25 % w/v Rochelle salt; 0.2 % w/v phenol; 0.05 % sodium metabisulphite) terminated the reaction, and the reactions were subsequently incubated for 10 min in rapidly boiling water [29]. Once cooled on ice, the OD_{575} was obtained using a Boeco S-22 UV/Vis spectrophotometer. The glucose amount (μg glucose ml^{-1}) released from CMC-Na^+ hydrolysis was extrapolated from a glucose standard curve. Soluble extracts from uninduced and untransformed cultures and resuspended pellets from all three conditions (induced empty vector, uninduced, untransformed) served as negative controls. Cellulase from *Trichoderma reesei* (Sigma Aldrich; 5 units/mg) served as the positive control.

2.6. Determination of optimal pH, sodium chloride concentration and temperature

Optimal parameters for CMC-Na^+ hydrolysis by the MBP-cellulase were determined by assaying 250 μg of soluble extracts in the presence of 0.5 % CMC-Na^+ at different temperatures, pH levels and NaCl concentrations for 1 h. For optimal pH determination, soluble protein extracts were incubated in different buffers over a pH range of 3–8. All buffers had a 50 mM concentration and included sodium citrate buffer (for pH 3–5) and sodium phosphate buffer (for pH 6–8) and were incubated at 50 °C. For optimal temperature determination, soluble protein extracts in sodium phosphate buffer (pH 6) were incubated at different temperatures (20–70 °C). In order to determine the optimal NaCl concentration for CMC-Na^+ hydrolysis, soluble protein extracts were incubated in the presence of increasing NaCl concentrations in the range of 0–1000 mM at 50 °C in sodium phosphate buffer (pH 6). All assays were performed as mentioned previously.

3. Results

3.1. Protein bioinformatics

A signal peptide which targets the cellulase for secretion from the cell, with a length of 17 amino acids (position 2–18) was identified, and subsequently omitted from the design and synthesis of the expression vector, pMAL-CGB E4160W. An automated homology model of the MBP-cellulase was constructed (Fig. 1) to computationally determine the impact of the MBP tag on the cellulase's structure, which could ultimately affect enzymatic function.

The estimated molecular weight of the MBP-cellulase, a fusion of the MBP tag (43 kDa) and a cellulase from *C. gattii* (47 kDa), is approximately 90 kDa. Additionally, the pI, extinction coefficient, aliphatic index, instability index and GRAVY values were found to be 4.97, 215090 M^{-1} cm^{-1}, 75.2, 25.24 and −0.477, respectively.

The pI, extinction coefficient, aliphatic index, instability index and GRAVY values of the cellulase without an N-terminal MBP are 4.57, 148990 M^{-1} cm^{-1}, 73.81, 31.84 and −0.417, respectively. The MBP-cellulase's higher aliphatic index suggest that fusion to the MBP tag increases the thermostability of the passenger cellulase whilst the lower GRAVY value of the fusion enzyme indicates that the MBP may increase the solubility of the cellulase enzyme [22,31].

3.2. Recombinant protein overexpression and purification

The 90 kDa MBP-cellulase, encoded on the pMAL-c5x vector, was successfully overexpressed in *E. coli* T7 at 16 °C using 0.2 mM IPTG and allowing induction to proceed for 24 h. A single-step purification of MBP-cellulase was subsequently carried out utilizing amylose resin in conjunction with gravity-flow chromatography to purify the fusion protein (Fig. 2).

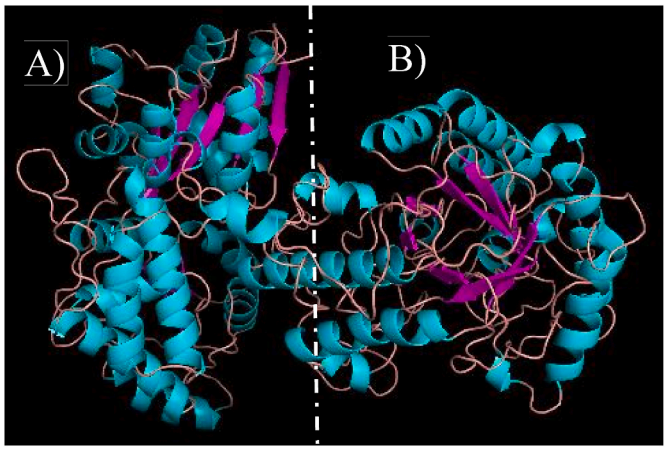

Fig. 1. Homology model representing the maltose binding protein-cellulase (MBP-cellulase) fusion protein constructed using Phyre2 [23]. A) represents the MBP tag and B) represents the cryptococcal cellulase. The fused cellulase still retains a typical $(\alpha/\beta)_8$ triose phosphate isomerase (TIM) barrel fold associated with glycosyl hydrolase family 5 (GH5) enzymes [30]. Alpha helices are represented by the colour cyan whilst magenta represents the fusion enzyme's beta-sheets. The automated homology model of MBP-cellulase was visualized using PyMOL [24].

Amylose affinity purification relies on the interactions between MBP and α-(1–4)-glycosidic linkages, such as those found in amylose and starch polymers [32]. Due to high affinity binding of maltose to MBP, maltose at a concentration of 10 mM can be used to efficiently elute MBP fusion enzymes from the amylose matrix [33].

Cleavage of the cryptococcal cellulase from the MBP tag using thrombin was not experimentally effective (data not shown), since there were still significant amounts of MBP-cellulase, which remained even when a buffer for optimal thrombin cleavage (20 mM Tris–HCl; pH 8.4; 150 mM NaCl; 25 mM CaCl2) was used [34].

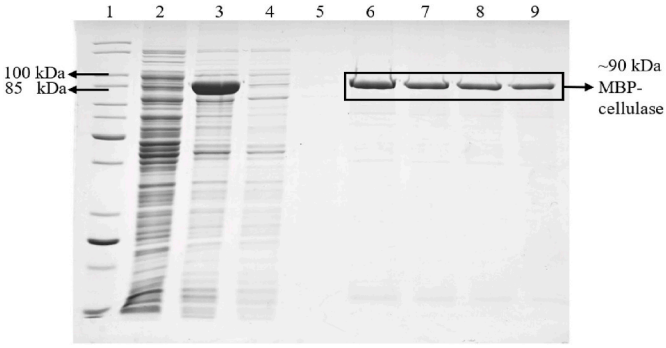

Fig. 2. Heterologous overexpression and single-step purification of MBP-cellulase fusion protein from soluble extracts of induced *Escherichia coli* T7 cells using amylose affinity chromatography. Lane 1: Unstained Protein Standard (New England Biolabs); lane 2: soluble extracts from untransformed *E. coli* T7 cells; lane 3: soluble extracts from induced *E. coli* T7 cells; lane 4: amylose column flow-through; lane 5: amylose column wash fraction; lanes 6–9: isocratic elutions of purified MBP-cellulase fusion protein.

3.3. Far-ultraviolet circular dichroism and intrinsic tryptophan fluorescence

The secondary structure of MBP-cellulase was interrogated using far-UV CD (Fig. 3A). The use of far-UV CD in the elucidation of a protein's secondary structure gives vital information regarding whether or not the protein is folded correctly and in the correct conformation [35]. Proteins which occur as aggregates tend to exhibit light scattering and a flattened CD spectra when compared to correctly folded proteins [36].

The tertiary structure of MBP-cellulase was also evaluated through the use of intrinsic tryptophan fluorescence (Fig. 3B). The analysis of a protein's tertiary structure using intrinsic tryptophan fluorescence provides valuable insights into a protein's conformation when its local environment is altered, for example in the presence of a ligand whose binding causes a perturbation in the protein's structure [37,38].

Conformational changes were induced in the presence of the cellulase's ligand, CMC-Na^+, or in the presence of a high concentration of a denaturant, such as urea, to induce unfolding (Fig. 3B) [37,39]. When denatured, MBP-cellulase produced a red-shift (increase in emission maximum) from 340 to 342 nm, which although minor, still represents a change in MBP-cellulase's conformation, and a drop in the fluorescence intensity from 918 to 535 absorbance units (A.U) (Fig. 3B, yellow line). A red-shift in the presence of 8 M urea indicates that the tryptophan residues are substantially exposed to the buffer environment, implying that MBP-cellulase has been entirely unfolded [40].

A blue-shift (decrease in emission maximum) and a decrease in fluorescence intensity occurred as a consequence of the MBP-cellulase's binding to a ligand, CMC-Na^+, (Fig. 3B, green line). Such an observation is indicative of an increase in hydrophobicity, which suggests that the tryptophan residues are less exposed to the buffer environment and become more buried within MBP-cellulase's core [41]. This observation is unsurprising, when considering that a change in the emission spectra of a particular protein is often linked to a conformational change due to pH shifts, changes in temperature and ligand binding [37].

3.4. Assaying soluble extracts for cellulase activity

The soluble extracts from a culture of *E. coli* T7 harbouring pMAL-CGB_E4160W induced with 0.2 mM IPTG was able to generate more glucose as a consequence of CMC-Na^+ hydrolysis, when compared to supernatants originating from cultures of untransformed and uninduced *E. coli* T7 cultures, as well as an induced culture harboring an empty pMAL vector (Fig. 4). There was a significant difference ($p < 0.01$) when the soluble extracts from induced cells harbouring pMAL-CGB_E4160W were incubated with CMC-Na^+, indicating the cellulolytic ability of MBP-cellulase.

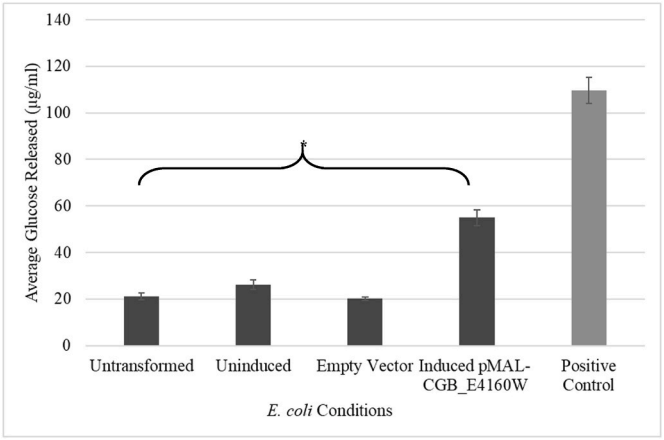

Fig. 4. Lysate productivity of four different *Escherichia coli* T7 strains (untransformed T7 cells, transformed uninduced cells, transformed induced T7 cells with an empty plasmid and transformed induced cells harbouring pMAL-CGB_E4160W) with respect to CMC-Na^+ hydrolysis based on the 3,5-dinitrosalicylic acid (DNS) assay (Miller, 1959). Error bars represent the standard deviation of three replicates (n = 3). There is a significant difference when comparing the three control conditions to the experimental, as evidenced by a p-value <0.01. One hundred units of cellulase derived from *Trichoderma reesei* served as the positive control.

The use of crude cell lysates or cell-free supernatants in the determination of enzyme activity is considered comparable to the use of purified protein [42], however using cell lysates facilitates more rapid determination of an enzyme's hydrolytic ability, without the need for time consuming purification processes.

3.5. Determination of optimal pH, sodium chloride concentration and temperature

The MBP-cellulase fusion enzyme displayed maximum activity at 50 °C (Fig. 5A) and retained over 50 % of its relative maximal activity at 60 °C. Additionally, the optimum pH of the MBP-cellulase was determined to be pH 6 (Fig. 5B) and the optimum NaCl concentration was found to be 500 mM (Fig. 5C) whilst retaining 80 and 60 % of its maximum activity at 750 and 1000 mM sodium chloride, respectively.

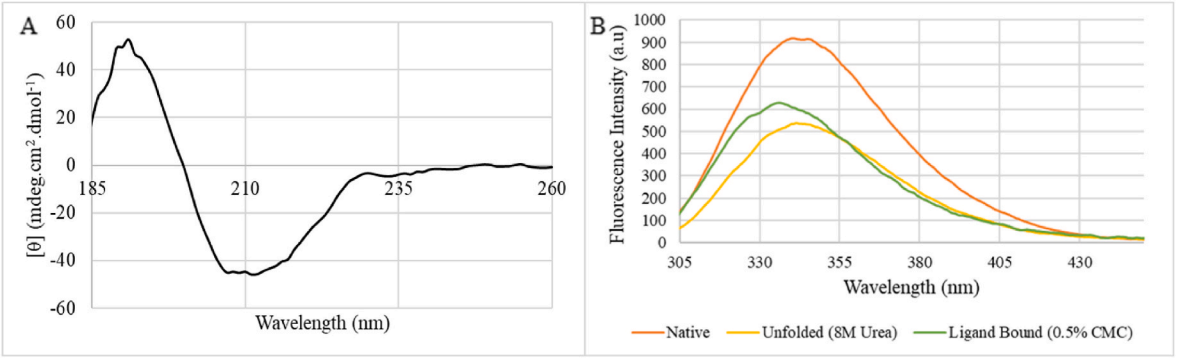

Fig. 3. A) Maltose binding protein-cellulase (MBP-cellulase; 10 μM) in 10 mM sodium phosphate buffer (pH 7) exhibits a dominant α-helical secondary structure due to the presence of a distinct peak at 190 nm and decline at 208 nm. A slight decline at 218 nm is indicative of β-sheets. **B)** Native MBP-cellulase (10 μM) (orange line) in sodium phosphate buffer (10 mM; pH 7) exhibited a high tryptophan fluorescent intensity emission at 340 nm. Denatured MBP-cellulase (10 μM) (yellow line) in sodium phosphate buffer (10 mM, pH 7) with 8 M urea exhibited a low tryptophan fluorescent intensity emission and red shift to 342 nm. Ligand binding with 0.5 % (w/v) carboxymethylcellulose (CMC; green line) resulted in a blue shift (emission at 335 nm) and lower fluorescent intensity which indicates increased hydrophobicity when compared to the native state (orange line).

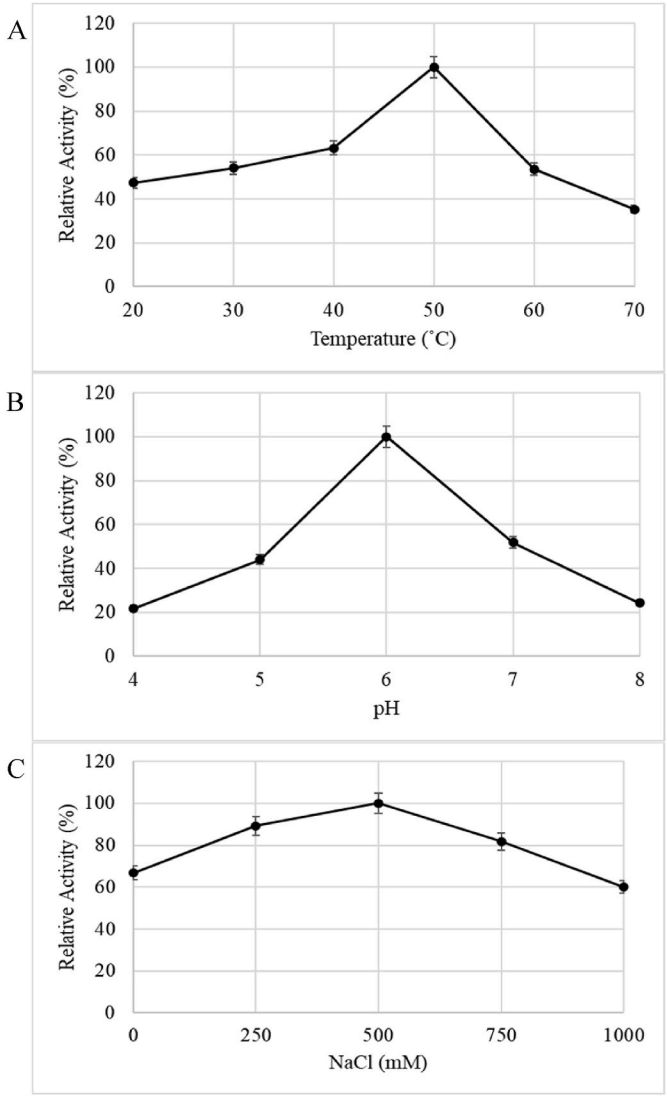

Fig. 5. A) Optimal temperature determination of maltose binding protein-cellulase using the 3,5-dinitrosalicylic acid (DNS) assay (Miller, 1959). The optimal temperature for MBP-cellulase was found to be 50 °C. **B)** Optimal pH determination of maltose binding protein-cellulase using the 3,5-dinitrosalicylic acid (DNS) assay. Citrate buffer 50 mM was used for pH 4–5 while 50 mM sodium phosphate buffer was used for pH 6–8. The optimal pH from enzymatic activity of maltose binding protein-cellulase (MBP-cellulase) was found to be 6. **C)** Optimal sodium chloride concentration determination of maltose binding protein-cellulase using the 3,5-dinitrosalicylic acid (DNS) assay. The optimal sodium chloride concentration was found to be 500 mM. All assays were carried out as previously described. Error bars represent the standard deviation of three replicates (n = 3).

4. Discussion

The medically relevant environmental yeast, *C. gattii*, is one of the primary aetiological agents of cryptococcosis [3]. The emerging drug resistance, pathogenesis and virulence factors of this yeast have been extensively studied and are well understood [4]. However, the environmental physiology of *C. gattii* and its true ecological niche are points of contention and remain unclear [43]. A novel gene derived from the sequenced genome of *C. gattii* WM276 was annotated as a putative cellulase [44]. To gain insights into the potential environmental metabolism of *C. gattii*, and elucidate the functionality of the cellulase protein, the gene, CGB_E4160W, was codon-optimized (with the signal peptide omitted) and cloned into a pMAL-c5x vector for recombinant overexpression in *E. coli* T7. The recombinant cellulase, overexpressed as a fusion protein with an N-terminal MBP, was predominantly present in the soluble fraction and was subsequently purified in a single step, using amylose affinity chromatography.

Computational data indicates that despite the presence of a large MBP tag, the cellulase component of the fusion enzyme should retain a typical $(\alpha/\beta)_8$ triose phosphate isomerase (TIM) barrel fold associated with glycosyl hydrolase family 5 (GH5) enzymes [30]. This predicted structure was subsequently confirmed using far-UV-CD, where MBP-cellulase exhibited a CD maximum at 190 nm and two CD minima at 208 nm and, to a lesser extent 218 nm (Fig. 3A). This suggests that the MBP-cellulase fusion enzyme is primarily α-helical, with the presence of some β-sheets [45]. The observed peaks are also consistent with the research of Pimentel and colleagues (2017), who determined that a GH5 endoglucanase generated from a metagenome library, had a CD maximum at 190 nm and two CD minima at 209 and 219 nm [46].

The theoretical parameters of MBP-cellulase collectively indicate that the cellulase is acid-tolerant, thermostable and hydrophobic. The thermostable nature of this enzyme make it a suitable candidate for utility in the textile and detergent industry [47], whilst this enzyme's acid-tolerant nature is advantageous in processes that necessitate acid pretreatment of lignocellulosic material, among which is the production of biofuels from agricultural residue [48].

Intrinsic tryptophan fluorescence was used to evaluate the tertiary structure of the MBP-cellulase [37]. Like other GH5 endoglucanases, in its native state the MBP-cellulase exhibited an emission maximum at 340 nm after initial excitation at 295 nm (Fig. 3B, orange line) [38,49]. In the denatured state (Fig. 3B, yellow line), the MBP-cellulase produces a red-shift, which indicates that the tryptophan residues are substantially exposed to the buffer environment, implying that MBP-cellulase has been entirely unfolded [40]. Finally, a blue-shift (decrease in emission maximum) and a decrease in fluorescence intensity occurred as a consequence of the MBP-cellulase's binding to CMC-Na^+, (Fig. 3B, green line), which indicates increased hydrophobicity, suggesting that the tryptophan residues are less exposed to the buffer environment and become more buried within MBP-cellulase's core [41], which is typical of conformational changes associated with ligand binding [50].

Despite its large molecular weight, the MBP tag does not seem to impede its passenger protein's enzymatic function, since MBP-cellulase displayed cellulolytic activity towards CMC-Na^+ (Fig. 4). Similarly, Jiménez-Guerrero and colleagues (2019) observed that a GH12 cellulase exhibited similar cellulase activity regardless of whether it was present as an MBP-cellulase fusion enzyme or a cleaved and untagged enzyme [51]. Moreover, an endo-acting xylanase, an endo-β-1,4-mannanase and a cellulase were able to retain their hydrolytic function when fused to an N-terminal MBP [52–54]. Midiri and co-workers (2020) were able to readily detect CMC hydrolysis from lysates of *E. coli* transformed with a pET-21b vector, harbouring a gene encoding a cellulase from *C. neoformans* [55]. This approach enables rapid determination of enzyme activity, and also mitigates the unpredictable loss of enzyme function and solubility, as a result of extended processing times during the purification process [56].

The optimal temperature of MBP-cellulase was found to be slightly higher than the reported temperature optima of a recombinant cellulase from *C. neoformans*, which was 37 °C [55]. This discrepancy is likely attributed to the fact that the MBP fusion tag is known to enhance the thermostability of its passenger protein [57]. Generally, however, GH5 cellulases have an optimal temperature of 50 °C [58–60]. The optimal pH was slightly higher than that reported in previous studies looking at cellulases from other cryptococcal species [55,61]. Thongekkaew and co-workers (2008) reported a pH optimum of 3.5 for a recombinant cellulase from *Cryptococcus* sp. S-2, whilst Midiri and co-workers (2020) reported a pH optimum of 4 for a recombinant cellulase from *C. neoformans*. Despite the minor discrepancy in optimal pH compared to other cryptococcal cellulases, cellulases derived from *Aspergillus fumigatus, Bacillus velezensis* and *Rhizopus oryzae* all exhibited an optimal pH

of 6 [62–64]. Lastly, a recombinant cellulase derived from *A. glaucus* was found to have a 220 % increase in activity when in the presence of 500 mM NaCl as compared to the absence of NaCl [65]. The halotolerant nature of this cellulase could make it an attractive target for industry as the pre-treatment of cellulosic biomass needs strong alkaline agents followed by acid neutralisation, which generates excessive salinity as a common consequence [66].

5. Conclusion

To the best of our knowledge, this work represents the first over-expression, purification, and characterization of a cellulase from *C. gattii*. Moreover, this is the first illustration of the structural character of a cellulase from any cryptococcal pathogen. Overall, these findings support the notion that woody material, is in fact, the true ecological niche of *C. gattii* since the presence of a functional cellulase enzyme suggests that this pathogen can colonize plant material, successfully hydrolysing cellulosic substrates for growth.

Funding

The authors declare that no funds, grants, or other support were received during the preparation of this manuscript.

Ethics approval

This article does not contain any studies with human participants or animals performed by any of the authors.

CRediT authorship contribution statement

Dylan Moodley: Writing – original draft, Methodology, Formal analysis, Data curation. **Angela Botes:** Writing – review & editing, Supervision, Project administration, Investigation, Funding acquisition, Conceptualization.

Declaration of competing interest

The authors have no competing interests to declare that are relevant to the content of this article.

Data availability

Data will be made available on request.

Acknowledgments

This work was supported by the University of the Witwatersrand, and the South African National Research Foundation. Dr. Ikechukwu Achilonu and The University of the Witwatersrand's Protein structure and function research unit are acknowledged for the use of their biophysical characterization facilities.

References

[1] M.A. Abegg, F.L. Cella, J. Faganello, et al., Cryptococcus neoformans and Cryptococcus gattii isolated from the excreta of psittaciformes in a southern Brazilian zoological garden, Mycopathologia 161 (2006) 83–91, https://doi.org/10.1007/s11046-005-0186-z.
[2] M.S. Lazéra, M.A. Cavalcanti, L. Trilles, et al., Cryptococcus neoformans var. gattii–evidence for a natural habitat related to decaying wood in a pottery tree hollow, Med. Mycol. 36 (1998) 119–122.
[3] S.C.-A. Chen, W. Meyer, T.C. Sorrell, Cryptococcus gattii infections, Clin. Microbiol. Rev. 27 (2014) 980–1024, https://doi.org/10.1128/CMR.00126-13.
[4] R. Watkins, J. King, S. Johnston, Nutritional requirements and their importance for virulence of pathogenic Cryptococcus species, Microorganisms 5 (2017) 65, https://doi.org/10.3390/microorganisms5040065.
[5] A. Chowdhary, H.S. Randhawa, A. Prakash, J.F. Meis, Environmental prevalence of *Cryptococcus neoformans* and *Cryptococcus gattii* in India: an update, Crit. Rev. Microbiol. 38 (2012) 1–16, https://doi.org/10.3109/1040841X.2011.606426.
[6] A.P. Litvintseva, I. Carbone, J. Rossouw, et al., Evidence that the human pathogenic fungus Cryptococcus neoformans var. grubii may have evolved in Africa, PLoS One 6 (2011) e19688, https://doi.org/10.1371/journal.pone.0019688.
[7] D.J. Springer, R.B. Billmyre, E.E. Filler, et al., Cryptococcus gattii VGIII isolates causing infections in HIV/AIDS patients in southern California: identification of the local environmental source as arboreal, PLoS Pathog. 10 (2014) e1004285, https://doi.org/10.1371/journal.ppat.1004285.
[8] T.J. Pfeiffer, D.H. Ellis, Environmental isolation of Cryptococcus neoformans var. gattii from Eucalyptus tereticornis, J. Med. Vet. Mycol. 30 (1992) 407–408.
[9] J.-M. Vreulink, T. Boekhout, H. Vismer, A. Botha, The growth of Cryptococcus gattii MATα and MATa strains is affected by the chemical composition of their woody debris substrate, Fungal Ecology 47 (2020) 100943, https://doi.org/10.1016/j.funeco.2020.100943.
[10] A. Botes, T. Boekhout, F. Hagen, et al., Growth and mating of Cryptococcus neoformans var. grubii on woody debris, Microb. Ecol. 57 (2009) 757–765, https://doi.org/10.1007/s00248-008-9452-1.
[11] K.-L. Min, Y.-H. Kim, Y.W. Kim, et al., Characterization of a novel laccase produced by the wood-rotting fungus phellinus ribis, Arch. Biochem. Biophys. 392 (2001) 279–286, https://doi.org/10.1006/abbi.2001.2459.
[12] A. Hansakon, P. Ngamskulrungroj, P. Angkasekwinai, Contribution of laccase expression to immune response against Cryptococcus gattii infection, Infect. Immun. 88 (2020) e00712, https://doi.org/10.1128/IAI.00712-19, 19.
[13] F. Ghaemi, L.C. Abdullah, H. Ariffin, Lignocellulose structure and the effect on nanocellulose production, in: Lignocellulose for Future Bioeconomy, Elsevier, 2019, pp. 17–30.
[14] A. Zoghlami, G. Paës, Lignocellulosic biomass: understanding recalcitrance and predicting hydrolysis, Front. Chem. 7 (2019) 874, https://doi.org/10.3389/fchem.2019.00874.
[15] F. Xu, Y. Li, Biomass digestion, in: Encyclopedia of Sustainable Technologies, Elsevier, 2017, pp. 197–204.
[16] D. Harris, V. Bulone, S.-Y. Ding, S. DeBolt, Tools for cellulose analysis in plant cell walls, Plant Physiol. 153 (2010) 420–426, https://doi.org/10.1104/pp.110.154203.
[17] Y. Siu-Rodas, M.D.L.A. Calixto-Romo, K. Guillén-Navarro, et al., Bacillus subtilis with endocellulase and exocellulase activities isolated in the thermophilic phase from composting with coffee residues, Rev. Argent. Microbiol. 50 (2018) 234–243, https://doi.org/10.1016/j.ram.2017.08.005.
[18] R.C. Kuhad, R. Gupta, A. Singh, Microbial cellulases and their industrial applications, Enzym. Res. (2011) 1–10, https://doi.org/10.4061/2011/280696, 2011.
[19] J.A. Langston, T. Shaghasi, E. Abbate, et al., Oxidoreductive cellulose depolymerization by the enzymes cellobiose dehydrogenase and glycoside hydrolase 61, Appl. Environ. Microbiol. 77 (2011) 7007–7015, https://doi.org/10.1128/AEM.05815-11.
[20] P.-Y. Cheng, A. Sham, J.W. Kronstad, *Cryptococcus gattii* isolates from the British columbia cryptococcosis outbreak induce less protective inflammation in a murine model of infection than *Cryptococcus neoformans*, Infect. Immun. 77 (2009) 4284–4294, https://doi.org/10.1128/IAI.00628-09.
[21] K. Guruprasad, B.V.B. Reddy, M.W. Pandit, Correlation between stability of a protein and its dipeptide composition: a novel approach for predicting *in vivo* stability of a protein from its primary sequence, Protein Eng. Des. Sel. 4 (1990) 155–161, https://doi.org/10.1093/protein/4.2.155.
[22] H.A. Rodríguez-Ruiz, O.L. Garibay-Cerdenares, B. Illades-Aguiar, et al., In silico prediction of structural changes in human papillomavirus type 16 (HPV16) E6 oncoprotein and its variants, BMC Mol and Cell Biol 20 (2019) 35, https://doi.org/10.1186/s12860-019-0217-0.
[23] L.A. Kelley, S. Mezulis, C.M. Yates, et al., The Phyre2 web portal for protein modeling, prediction and analysis, Nat. Protoc. 10 (2015) 845–858, https://doi.org/10.1038/nprot.2015.053.
[24] S. Yuan, H.C.S. Chan, Z. Hu, Using PyMOL as a platform for computational drug design, WIREs Comput Mol Sci 7 (2017) e1298, https://doi.org/10.1002/wcms.1298.
[25] A. Froger, J.E. Hall, Transformation of plasmid DNA into E. coli using the heat shock method, JoVE 253 (2007), https://doi.org/10.3791/253.
[26] U.K. Laemmli, Cleavage of structural proteins during the assembly of the head of bacteriophage T4, Nature 227 (1970) 680–685, https://doi.org/10.1038/227680a0.
[27] A.J. Miles, B.A. Wallace, Synchrotron radiation circular dichroism spectroscopy of proteins and applications in structural and functional genomics, Chem. Soc. Rev. 35 (2006) 39–51, https://doi.org/10.1039/B316168B.
[28] S. Kelly, N. Price, The use of circular dichroism in the investigation of protein structure and function, CPPS 1 (2000) 349–384, https://doi.org/10.2174/1389203003381315.
[29] G.L. Miller, Use of dinitrosalicylic acid reagent for determination of reducing sugar, Anal. Chem. 31 (1959) 426–428, https://doi.org/10.1021/ac60147a030.
[30] R.K. Wierenga, The TIM-barrel fold: a versatile framework for efficient enzymes, FEBS (Fed. Eur. Biochem. Soc.) Lett. 492 (2001) 193–198, https://doi.org/10.1016/S0014-5793(01)02236-0.
[31] A. Ikai, Thermostability and aliphatic index of globular proteins, J. Biochem. 88 (1980) 1895–1898.

[32] R. Dippel, W. Boos, The maltodextrin system of *Escherichia coli* : metabolism and transport, J. Bacteriol. 187 (2005) 8322–8331, https://doi.org/10.1128/JB.187.24.8322-8331.2005.
[33] S. Szmelcman, M. Schwartz, T.J. Silhavy, W. Boos, Maltose transport in Escherichia coli K12. A comparison of transport kinetics in wild-type and lamba-resistant mutants with the dissociation constants of the maltose-binding protein as measured by fluorescence quenching, Eur. J. Biochem. 65 (1976) 13–19, https://doi.org/10.1111/j.1432-1033.1976.tb10383.x.
[34] D. Liu, R. Xu, K. Dutta, D. Cowburn, N-terminal cysteinyl proteins can be prepared using thrombin cleavage, FEBS (Fed. Eur. Biochem. Soc.) Lett. 582 (2008) 1163–1167, https://doi.org/10.1016/j.febslet.2008.02.078.
[35] N.J. Greenfield, Using circular dichroism spectra to estimate protein secondary structure, Nat. Protoc. 1 (2006) 2876–2890, https://doi.org/10.1038/nprot.2006.202.
[36] Venyaminov Syu, J.T. Yang, Determination of protein secondary structure, in: G. D. Fasman (Ed.), Circular Dichroism and the Conformational Analysis of Biomolecules, Springer US, Boston, MA, 1996, pp. 69–107.
[37] A. Ghisaidoobe, S. Chung, Intrinsic tryptophan fluorescence in the detection and analysis of proteins: a focus on förster resonance energy transfer techniques, IJMS 15 (2014) 22518–22538, https://doi.org/10.3390/ijms151222518.
[38] T.V. Souza, J.N. Araujo, V.M. Da Silva, et al., Chemical stability of a cold-active cellulase with high tolerance toward surfactants and chaotropic agent, Biotechnology Reports 9 (2016) 1–8, https://doi.org/10.1016/j.btre.2015.11.001.
[39] O.I. Povarova, I.M. Kuznetsova, K.K. Turoverov, Differences in the pathways of proteins unfolding induced by urea and guanidine hydrochloride: molten globule state and aggregates, PLoS One 5 (2010) e15035, https://doi.org/10.1371/journal.pone.0015035.
[40] M. Balsera, M. Menéndez, J.L. Sáiz, et al., Structural stability of the PsbQ protein of higher plant photosystem II, Biochemistry 43 (2004) 14171–14179, https://doi.org/10.1021/bi048369e.
[41] A. Dusa, J. Kaylor, S. Edridge, et al., Characterization of oligomers during α-synuclein aggregation using intrinsic tryptophan fluorescence, Biochemistry 45 (2006) 2752–2760, https://doi.org/10.1021/bi051426z.
[42] D.C. Garcia, B.P. Mohr, J.T. Dovgan, et al., Elucidating the potential of crude cell extracts for producing pyruvate from glucose, Synthetic Biology 3 (2018) ysy006, https://doi.org/10.1093/synbio/ysy006.
[43] H.M. Edwards, M. Cogliati, G. Kwenda, M.C. Fisher, The need for environmental surveillance to understand the ecology, epidemiology and impact of *Cryptococcus* infection in Africa, FEMS (Fed. Eur. Microbiol. Soc.) Microbiol. Ecol. 97 (2021) fiab093, https://doi.org/10.1093/femsec/fiab093.
[44] C.A. D'Souza, J.W. Kronstad, G. Taylor, et al., Genome variation in Cryptococcus gattii, an emerging pathogen of immunocompetent hosts, mBio 2 (2011) e00342, https://doi.org/10.1128/mBio.00342-10, 10.
[45] D.H. Corrêa, C.H. Ramos, The use of circular dichroism spectroscopy to study protein folding, form and function, Afr. J. Biochem. Res. 3 (2009) 164–173.
[46] A.C. Pimentel, G.C.G. Ematsu, M.V. Liberato, et al., Biochemical and biophysical properties of a metagenome-derived GH5 endoglucanase displaying an unconventional domain architecture, Int. J. Biol. Macromol. 99 (2017) 384–393, https://doi.org/10.1016/j.ijbiomac.2017.02.075.
[47] R. Kinet, J. Destain, S. Hiligsmann, et al., Thermophilic and cellulolytic consortium isolated from composting plants improves anaerobic digestion of cellulosic biomass: toward a microbial resource management approach, Bioresour. Technol. 189 (2015) 138–144, https://doi.org/10.1016/j.biortech.2015.04.010.
[48] N. Mosier, Features of promising technologies for pretreatment of lignocellulosic biomass, Bioresour. Technol. 96 (2005) 673–686, https://doi.org/10.1016/j.biortech.2004.06.025.
[49] P. Sharma, P. Guptasarma, Endoglucanase activity at a second site in *Pyrococcus furiosus* triosephosphate isomerase—promiscuity or compensation for a metabolic handicap? FEBS Open Bio 7 (2017) 1126–1143, https://doi.org/10.1002/2211-5463.12249.
[50] M. Möller, A. Denicola, Protein tryptophan accessibility studied by fluorescence quenching, Biochem. Mol. Biol. Educ. 30 (2002) 175–178, https://doi.org/10.1002/bmb.2002.494030030035.
[51] I. Jiménez-Guerrero, F. Pérez-Montaño, A. Zdyb, et al., GunA of Sinorhizobium (Ensifer) fredii HH103 is a T3SS-secreted cellulase that differentially affects symbiosis with cowpea and soybean, Plant Soil 435 (2019) 15–26, https://doi.org/10.1007/s11104-018-3875-3.
[52] K.L. Braithwaite, G.W. Black, G.P. Hazlewood, et al., A non-modular endo- β -1,4-mannanase from *Pseudomonas fluorescens* subspecies *cellulosa*, Biochem. J. 305 (1995) 1005–1010, https://doi.org/10.1042/bj3051005.
[53] S. Jindou, Q. Xu, R. Kenig, et al., Novel architecture of family-9 glycoside hydrolases identified in cellulosomal enzymes of *Acetivibrio cellulolyticus* and *Clostridium thermocellum*, FEMS (Fed. Eur. Microbiol. Soc.) Microbiol. Lett. 254 (2006) 308–316, https://doi.org/10.1111/j.1574-6968.2005.00040.x.
[54] M. Mitreva-Dautova, E. Roze, H. Overmars, et al., A symbiont-independent endo-1,4-β-xylanase from the plant-parasitic nematode *Meloidogyne incognita*, MPMI (Mol. Plant-Microbe Interact.) 19 (2006) 521–529, https://doi.org/10.1094/MPMI-19-0521.
[55] A. Midiri, G. Mancuso, G. Lentini, et al., Characterization of an immunogenic cellulase secreted by Cryptococcus pathogens, Med. Mycol. 58 (2020) 1138–1148, https://doi.org/10.1093/mmy/myaa012.
[56] E. Dako, A.-M. Bernier, A. Thomas, K. C, The problems associated with enzyme purification, in: D. Ekinci (Ed.), Chemical Biology, InTech, 2012.
[57] E.R. LaVallie, E.A. DiBlasio, S. Kovacic, et al., A thioredoxin gene fusion expression system that circumvents inclusion body formation in the E. coli cytoplasm, Nat. Biotechnol. 11 (1993) 187–193, https://doi.org/10.1038/nbt0293-187.
[58] M. Junghare, T. Manavalan, L. Fredriksen, et al., Biochemical and structural characterisation of a family GH5 cellulase from endosymbiont of shipworm P. megotara, Biotechnol. Biofuels 16 (2023) 61, https://doi.org/10.1186/s13068-023-02307-1.
[59] A. Maharjan, B. Alkotaini, B.S. Kim, Fusion of carbohydrate binding modules to bifunctional cellulase to enhance binding affinity and cellulolytic activity, Biotechnol Bioproc E 23 (2018) 79–85, https://doi.org/10.1007/s12257-018-0011-4.
[60] F. Zheng, J.V. Vermaas, J. Zheng, et al., Activity and thermostability of GH5 endoglucanase chimeras from mesophilic and thermophilic parents, Appl. Environ. Microbiol. 85 (2019) e02079, https://doi.org/10.1128/AEM.02079-18, 18.
[61] J. Thongekkaew, H. Ikeda, K. Masaki, H. Iefuji, An acidic and thermostable carboxymethyl cellulase from the yeast Cryptococcus sp. S-2: purification, characterization and improvement of its recombinant enzyme production by high cell-density fermentation of Pichia pastoris, Protein Expr. Purif. 60 (2008) 140–146, https://doi.org/10.1016/j.pep.2008.03.021.
[62] P. Saroj, M. P, K. Narasimhulu, Biochemical characterization of thermostable carboxymethyl cellulase and β-glucosidase from Aspergillus fumigatus JCM 10253, Appl. Biochem. Biotechnol. 194 (2022) 2503–2527, https://doi.org/10.1007/s12010-022-03839-2.
[63] M. Karmakar, D. Lahiri, M. Nag, et al., Purification, characterization, and application of endoglucanase from Rhizopus oryzae as antibiofilm agent, Appl. Biochem. Biotechnol. 195 (2023) 5439–5457, https://doi.org/10.1007/s12010-022-04043-y.
[64] Y. Liu, H. Guo, Y. Wu, W. Qin, Purification and characterizations of a novel recombinant Bacillus velezensis endoglucanase by aqueous two-phase system, Bioresour Bioprocess 5 (2018) 19, https://doi.org/10.1186/s40643-018-0204-x.
[65] Z. Li, X. Pei, Z. Zhang, et al., The unique GH5 cellulase member in the extreme halotolerant fungus Aspergillus glaucus CCHA is an endoglucanase with multiple tolerance to salt, alkali and heat: prospects for straw degradation applications, Extremophiles 22 (2018) 675–685, https://doi.org/10.1007/s00792-018-1028-5.
[66] H.B. Klinke, A.B. Thomsen, B.K. Ahring, Inhibition of ethanol-producing yeast and bacteria by degradation products produced during pre-treatment of biomass, Appl. Microbiol. Biotechnol. 66 (2004) 10–26, https://doi.org/10.1007/s00253-004-1642-2.